Electronic Supplementary Information

A Water-Soluble Temperature nanoProbe based on a Multimodal Magnetic-Luminescent nanoColloid

*Shu Chen, Clare Hoskins, Lijun Wang, Michael P. MacDonald, and Pascal André **

* Pascal.Andre@st-andrews.ac.uk

SI-I. Synthetic Pathways

SI-I.1. Materials

All chemical reagents, unless otherwise stated, were purchased from Sigma, used without further purification but degassed before use: Disodium tetracarbonylferrate-dioxane complex ($Na_2Fe(CO)_4$•1.5 $C_4H_8O_2$), platinum(II) acetylacetonate ($Pt(acac)_2$, 97 %), oleylamine (70 %), oleic acid (90 %), cysteamine (CA, $HSCH_2CH_2NH_2$, BioChemika, ≥ 98.0 %), tetraethylorthosilicate (TEOS, $Si(OC_2H_5)_4$, GC, ≥ 99.0 %), Tetramethyl rhodamine isothiocyanate (TRITC, SI-Figure 1), (3-amino propyl)triethoxysilane (APTES, $H_2N(CH_2)_3Si(OC_2H_5)_3$, ≥ 98 %), IGEPAL® CO-520 (NP-5, $(C_2H_4O)_n$•$C_{15}H_{24}O$, n ~ 5). When available ACS grade was chosen to select the solvents: dibenzyl ether (≥ 98.0 %), hexane (99.0 %), ethanol (≥ 99.5 %), chloroform (≥ 99 %, anhydrous), methanol (≥ 99.8 %), cyclohexane (GC, ≥ 98.0 %), ammonium hydroxide aqueous solution (NH_4OH, 28.0 - 30.0 %).

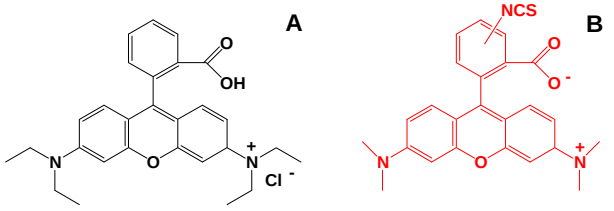

SI-Figure 1. Molecular structure of Rhodamine B (A) and tetramethylrhodamine isothiocyanate, TRITC (B).

SI-I.2. Protocols

FePt nPs synthesis: Several chemical pathways have been developed to synthesize FePt MnPs in aqueous and inorganic media, most often leading to an fcc- crystalline structure.[1] All the syntheses were carried out inside a glove box. A solution made of $Pt(acac)_2$ (1 mmol), oleyl amine (8 mmol) and oleic acid (4 mmol) in 10 mL of dibenzyl ether was placed in a 50 mL round bottom flask connected to a condenser. A separate solution of $Na_2Fe(CO)_4$ (1 mmol) in 10 mL dibenzyl ether was prepared also stirred at 100 °C for 1 h and still under stirring, both solutions were heated up to 100 °C for 1 h to remove oxygen and moisture. The two solutions were then mixed together and heated up to 150 °C with a heating rate of 15 °C/min. After 1h, the mixture was further heated up to reflux ~ 300 °C for 3 h. The reaction was then stopped, and the dark solution cooled down to room temperature. The nPs were then precipitated by addition of ethanol and centrifugation. The supernatant was discarded, while the sediment was dispersed in hexane, and precipitated one more time with ethanol and centrifugation.[1q,2]

FePt ligand exchange: Ligand exchange experiments were carried out in a glove box according to a modified protocol based on the literature [3]. For a typical experiment, 30 mL hexane was added into 3 mL (13.5 mg/mL) of as-synthesized oleic acid/ oleylamine coated fcc-FePt hexane solution. To remove the excess of ligands, the nPs were precipitated by addition of 60 mL ethanol and collected by centrifugation. The nPs were redispersed in 15 mL of chloroform assisted with sonication. 15 mL of cysteamine in methanol solution (0.5 M) was added dropwise to the FePt nPs/$CHCl_3$ mixture under vigorous stirring. The final solution was left under stirring for 48 h to complete the ligand exchange. To extract the nPs, they were redispersed in 10 mL ethanol and sonicated, 20 mL hexane was added and the solution was centrifuged. This process was repeated twice to remove $CHCl_3$, methanol and the excess of ligands. The nPs were then redispersed in 10 mL ethanol and 20 mL deionized water mixture, sonicated and collected by centrifugation. This step was repeated 6 times to obtain positively charged nPs stable in deionized water for more than 8 months.

FePt-silica: The FePt-silica MnPs were prepared by hydrolysis of tetraethylorthosilicate (TEOS) and the silica shell surface was further functionalized with (3-aminopropyl) triethoxysilane.[4] Reverse microemulsions were prepared by mixing under vigorous stirring 10 mL cyclohexane, 1.3 mL NP-5 and 50 µL DI H_2O. 2 mg (~ 3-4 nmol) of FePt MnPs were then dispersed in 1 mL cyclohexane and added dropwise into the reverse microemulsion. After 15 min, 80 µL TEOS was also added dropwise. After another 15 min, 150 µL $NH_4.H_2O$ (28-30 %) was added dropwise. The solution was kept under constant stirring at for 72 h. To form amine functionalized FePt-SiO_2 MnPs, 100 µL of APTES was added after 48 h and kept stirring for another 24 h. The nPs were precipitated by centrifugation after addition of 3 mL of ethanol and 2 mL of methanol. The nPs were redispersed in 5 mL of ethanol and precipitated by centrifugation after addition of 10 mL of hexane. This step was repeated up to 6 times to completely remove the surfactant. FePt-SiO_2 nPs were stable both in ethanol and DI water, while FePt-SiO_2 nPs were stable in deionized water.

Noticeably, the protocol associated with the silica coating can

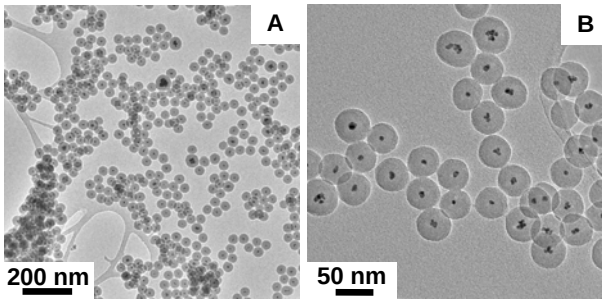

SI-Figure 2. TEM images of FePt coated with a silica shell: low magnification (A), higher magnification (B).

be tuned to provide homogeneous SiO_2 shell as illustrated by the Low magnification TEM image in SI-Figure 2A. In addition, careful control of the experimental condition can prevent the formation of silica nPs without any FePt as illustrated in SI-Figure 2B.

FePt/SiO_2/TRICT-SiO_2/APTES nPs: 15 µL of TEOS was injected after the dispersion of FePt nPs in a reverse microemulsion by following same procedure as the preparation of FePt-silica nPs (see above). The reaction was kept under stirring for 24 h to allow pre-growing of a thin layer of silica shell around the FePt core. A mixture contains ~ 60 µL TEOS and ~ 90 µL 1 mg/mL TRITC (Tetramethyl rhodamine isothiocyanate) ethanol solution was injected dropwise into the reaction system and kept stirring for 48 h.[5] To form amine functionalized FePt/SiO_2/TRICT-SiO_2 nPs, 100 µL of APTES was added after 48 h and kept stirring for another 24 h until the surface of the nanocolloids was completely passivated. nPs were washed and collected following the same protocol as described above for the FePt-SiO_2 nPs.

SI-II. Experimental Techniques

SI-II.1. Electron Microscopy

Transmission electron microscopy (TEM) images were recorded using a Gatan CCD camera on a JEOL JEM-2011 electron microscope operating at 200 kV.

The chemical composition of FePt nPs was examined with energy-dispersive X-ray spectroscopy (EDX) using an Oxford Link system installed in the JEM-2011 microscope.

SI-II.2. X-Ray Diffraction

Wide-angle powder X-ray diffraction (XRD) data were collected on a Stoe STADI/P powder diffractometer operating in transmission mode and with a small angle position sensitive detector. Incident radiation was generated using a $Fe_{K\alpha 1}$ source (λ=1.936 Å).

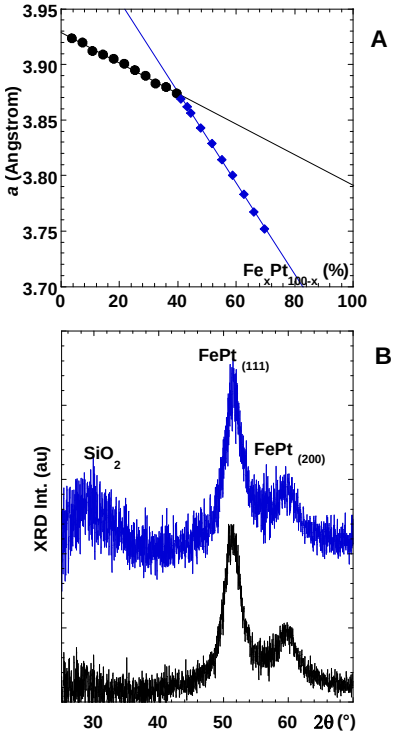

SI-Figure 3. FePt lattice constant (a) analysed by XRD vs. composition curve reported by Bonakdarkpour et al.[6] XRD patterns of FePt nPs (B-bottom), FePt-SiO_2 nPs (B-top).

The strongest (111) peak was fitted with Lorentzian-shaped peaks using STOEwinXpow and Kaleida-Graph softwares to precisely determine the diffraction peak positions. The crystalline grain size, D_{XRD}, of the FePt nPs was calculated according to Scherrer's formula presented in SI-eq. 1.[7]

$$D_{XRD} = \frac{0.9\lambda}{B\cos\theta} \qquad \text{(SI-eq. 1)}$$

where D_{XRD} is the " average" dimension of the crystallites, λ is the wavelength of the X-ray source (for Fe source is equal to 0.193604 nm), B is the full width at half maximum of the peak intensity, θ is the glancing angle.

The atomic composition of FePt MnPs was calculated based on the linear relations between lattice constant, a, and Fe percentage, Fe %, reported by Bonakdarkpour et al.[6] and presented in SI-Figure 3A, from which the following equations can be obtained:

$x_{\%Fe} < 40\ \%$ $\quad a = -0.0014\ x_{\%Fe} + 3.929$ (SI-eq. 2)

$x_{\%Fe} > 40\ \%$ $\quad a = -0.0041\ x_{\%Fe} + 4.039$ (SI-eq. 3)

SI-Figure 3B show peaks around 51° and 60° characteristic of *fcc*-FePt (111) and (200) peaks, respectively. The (111) peak position suggests that the nPs composition lays between 40 to 45 % of Fe. For the silica coated nPs, SiO_2 XRD characteristic peak is observed at ~28° (SI-Figure 3B-top blue curve). The crystal size is ~3.6 nm for both FePt and FePt-silica nPs.

SI-II.3. Magnetic Characterisation

SQUID: A 5.0 Tesla Superconducting Quantum Interference Device (SQUID) from Quantum Design (MPMS XL^{TM}) was used to characterize the nPs magnetic properties.

The nPs were dispersed in a polyvinylpyrrolidone matrix ($V_{Polymer}/V_{nPs}$ = 20) to prevent interaction between the nPs while the resulting sample was loaded into a low background gelatin capsule. Zero-Field Cooled and Field Cooled (ZFC/FC) measurements (SI-Figure 4A) were completed as follow: the sample was first cooled from room temperature to 2 K without any external field, next a small field 100 Oe was applied and the nPs magnetization was recorded as the temperature was increased up 275 K. The FC curve was obtained by cooling the sample back to 2 K exposed a 100 Oe magnetic field. The magnetization was

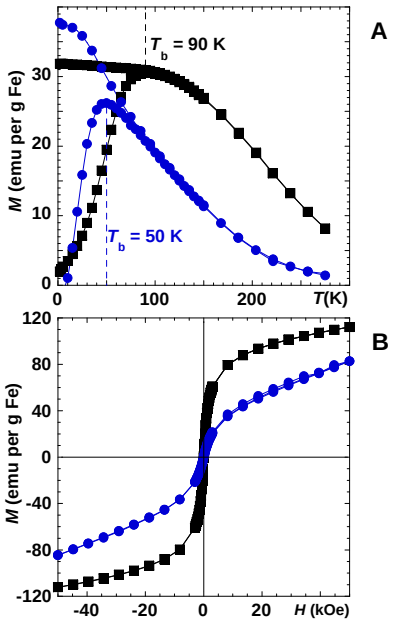

SI-Figure 4. ZFC-FC (A) and 300 K hysteresis (B) curves of FePt coated with cysteamine (■) and silica shell (●).

SI-Table 1. SQUID data of the FePt nPs. T_b is blocking temperature, M_s is the saturation moment of the nPs.

Samples	T_b (K)	M_s @ 300 K (emu per g of Fe)
FePt-CystA	90	112
FePt-SiO_2	50	83

then measured while the temperature was increased up to 275 K. Hysteresis measurements were completed at 300 K (SI-Figure 4B). The magnetization of the gelatine capsules and the PVP matrix was subsequently subtracted. The alteration of the magnetic properties of the nPs after silica coating (SI-Figure 4, SI-Table 1) can be attributed to the formation of thin layers of iron oxide or iron silicide resulting in the reduction of the magnetic effective volume and/or an alteration of the material. In support of this interpretation, the strong base environment associated with the silica coating can partially oxidize the FePt surface resulting in a thin layer of softer magnetic material like iron oxide or iron silicide, which because of its thinness is not visible by XRD or TEM.[8]

Magnetic Resonance Imaging (MRI): MRI characterisation of FePt-SiO_2 MnPs has been reported in ref. 9 showing that such MnPs were displaying strong MRI contrast agent properties.

SI-II.4. Toxicity: Trypan Blue Exclusion Assay

Whilst toxicity data have initially been puzzling, with for instance FePt being used to release apparent toxic components for cancer treatment,[11,10] it has recently been shown that FePt MnPs could be prepared as a non-toxic material above clinically relevant concentrations.[9]

In the present study, low concentration solutions of hybrid nanocolloids in MCF-7 and A375M cells (SI-Figure 5A-B) were used to confirm that, even with the dye inserted in the nanocolloids, the silica remained the material of choice to insulate substances, which could be harmful. Higher concentration of FePt-SiO_2 nPs in A375M where shown not to be toxic (SI-Figure 5C).

Cell viability was determined using trypan blue exclusion assay (Invitrogen, UK). Briefly human breast adenocarcinoma (MCF-7) and human melanoma (A375M) cells were seeded in a 12 well plate and incubated for 24 h at 37 ˚C with 5 % CO_2. The cells were treated with increasing concentrations of hybrid nanocolloid solutions (1.25 - 10 µg/mL) and incubated for specific time intervals. The cells were then washed with PBS three times and trypsinised. Trypan blue was added to 100 µL cell suspension in equal volume and incubated for 5 min at room temperature. The viable cells were counted using a CountessTM automated cell counter (Invitrogen, UK). Values of viability of treated cells were expressed as percentage of that from corresponding control cells. All experiments were repeated at least three times.

SI-Figure 5 shows the cell viability data of the FePt nanocolloids. In general all particles appeared to exhibit little cytotoxic effect when incubated with MCF-7 (SI-Figure 5A) and A375M (SI-Figure 5B) cell lines. After 7 day incubation with 10 µg/mL hybrid nanocolloid solutions, the total viability is reduced to 75 % and 85 % for MCF-7 and A375M, respectively. Lower cytotoxicity could certainly be achieved by increasing the outer silica layer as illustrated in SI-Figure 5C, showing that FePt nanoparticles coated with SiO_2 do not present any toxicity even though their concentration was increased up to 200 µg/mL and the toxicity monitored up to 7 days.

These results are in good agreement with our previous investigation in which a careful toxicity study was completed as a function of time, cell line (A375M, MCF and U2OS cells), and nPs concentration, and which demonstrated that FePt nP could be made non-toxic, used for cellular imaging and in-vivo MRI enhanced applications, hence opening the way for several future applications of FePt nPs, including regenerative medicine and stem cell therapy in addition to MR diagnostic imaging.[9]

These present results are consistent with fluorescent core-shell silica nanoparticles being reported as nontoxic at biologically relevant concentrations, hence, allowing their use for standard imaging applications including intravital visualization of capillaries and macrophages, sentinel lymph node mapping, and peptide-mediated multicolor cell labeling for real-time imaging of tumor metastasis and tracking of injected bone marrow cells in mice.[11] While a very important point, this is not unexpected considering that SiO_2 is being extensively used to make inorganic nanoparticles non-toxic.[12]

Nonetheless, these elements fully justify that, in the present research, multifunctional nPs were developed with an architecture including an SiO_2 shell, not only to guaranty the nanocolloids are non-toxic, but also to minimise the potential leakage of the dye from the magnetic core as well as to guaranty that the local temperature probe has a minimal exposure to local environmental parameters, such as viscosity or pH, which otherwise could prevent absolute fluorescence life-time and consequently temperature measurements.

SI-II.5. Optical Spectroscopy

The photoluminescent properties of solution of the multimodal hybrid nanocolloids were compared to solution of Rhodamine B and tetramethylrhodamine isothiocyanate (TRITC) which chemical structures are illustrated in SI-Figure 1. The samples were diluted in H_2O (bi-distilled) and their concentration was adjusted to reach a suitable optical density (OD_{max} < 0.15). All the optical measurements were made on a temperature controlled Edinburgh Instruments FLSP920 with double grating excitation

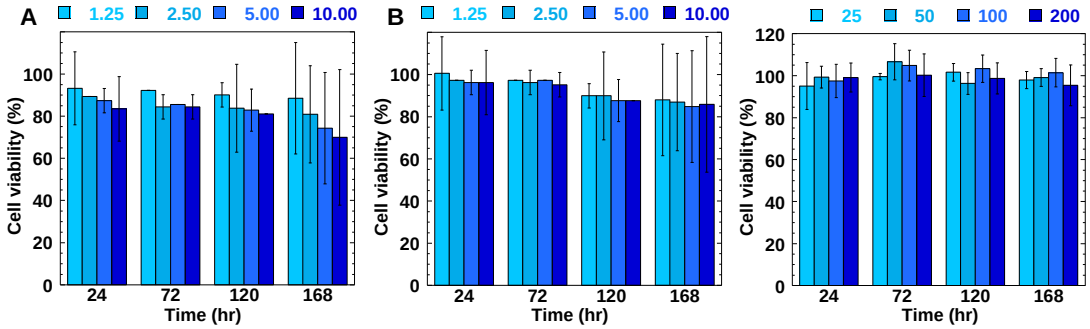

SI-Figure 5. Cell viability determined by Trypan blue exclusion of MCF-7 (A) and A375M (B, C) cells incubated with FePt-SiO_2-TRITC (A, B) and FePt-SiO_2 hybrid nanocolloids as a function of time and concentration in µg/mL (n=3 ± SD).

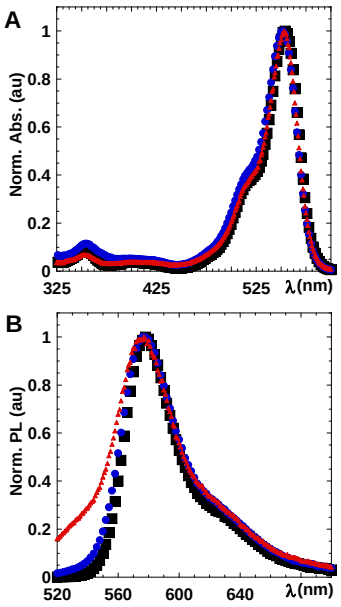

SI-Figure 6. Room temperature steady-state absorbance (A) and photoluminescence spectra (B) of Rhodamine B (■), TRICT (●) and FePt MnPs coated with silica shell and TRICT (▲) in aqueous solution.

and emission monochromators:

- The steady-state measurements (SI-Figure 6) were performed with the standard Xe900 450 W continuous xenon lamp for sample excitation and the standard red cooled PMT for photon detection.
- The lifetime measurements were completed in TCSP mode with a time range from 0 to 50 ns. The instrument was equipped with the EPL470 (λ = 470 nm, ν = 2 MHz) light source and MCP-PMT (Hamamatsu R3809U-50) detector. For all the samples, the emission wavelength was set at 578 nm, used a 200 – 900 nm grating, a 55 ° polarizer, and a 515 nm cut-off filter.

All the other parameters are given in SI-Table 2.

The photoluminescence (PL) decays were fitted by a single or double exponential model using a nonlinear least squares procedure:[13]

$$I(t) = \sum \alpha_i \exp\left(-t/\tau_{PLi}\right) \qquad \text{(SI-eq. 4)}$$

where $I(t)$ is the photoluminescence intensity as a function of time, τ_{PL} is the PL decay time and α is the pre-exponential factor associated with each decay time. α represents the amplitude of the components at t=0 and $\Sigma\alpha_i$ are normalized to unity.

SI-Table 2. Lifetime and measurement parameters.

Sample	Rhod. B	TRICT	FePt-SiO_2-TRICT
Channel Range	0 to 4095	0 to 4095	0 to 2047
$t_{calibration}$ (ns)	0.012	0.012	0.020
$BW_{emission}$ (nm)	10	10	24

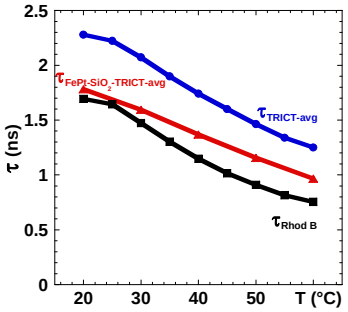

SI-Figure 7. PL decays measured in aqueous solution as a function of temperature: Rhodamine B (■), TRICT (●), FePt MnPs coated with silica shell and TRICT (▲).

SI-Table 3. In aqueous solution: Absorbance peak, position of the first photoluminescence peaks and associated spectral shift between the absorbance and PL peaks, fluorescence full width at half-maximum (δ_{PL}) and at 10%-maximum (δ_{PL10}), photo-luminescence decay and associated amplitude of the fit (τ_{PL}, α), average decay (τ_{avg}) at room temperature, temperature variation of the photoluminescence average decay.

Sample	Rhod. B	TRICT	FePt-SiO_2-TRICT
Abs. Peak (nm)	554	554	554
1st PL peak (nm)	578	578	577
Abs-PL shift (nm/cm^{-1})	24 / 749	24 / 749	23 / 719
δ_{PL} (nm/cm^{-1})	40 / 1232	45 / 1174	49 / 1467
δ_{PL10} (nm/cm^{-1})	110 / 1515	121 / 3367	155 / 4593
τ_{avg} (ns)	1.70	2.28	1.78
$\Delta\tau_{avg}$ (ps/°C)	26	28	20

In case of a double exponential decay, the lifetime weighted quantum yield, also called average lifetime, is defined in SI-eq. 5, [13] and plotted in SI-Figure 7.

$$\tau_{avg} = \sum \alpha_i \tau_{PLi} \qquad \text{(SI-eq. 5)}$$

SI-II.6. Summary and Effect of the Environment on Rhod. B PhotoLuminescence Lifetimes

SI-Table 3 presents a summary of the main characteristics of the Rhodamine derivatives used in this study.

a) absorbance and PL peaks do not shift,

b) the PL spectrum structure of the dye molecule is preserved even though the width of the PL increases from Rhod. B to the hybrid nanocolloids,

c) PL spectra are broader (larger full width at half maximum, δ_{PL}, as well as larger tailing, as shown by the δ_{PL10} values.

d) spectral shifts between the absorbance and PL peaks are constant.

While further examples can certainly be found in the literature, the SI-Table 4 below illustrates the effect on the environment on the photoluminescence life-time of Rhodamine-B.

SI-Table 4. Rhodamine B PL lifetime in various environment.

Solvents	τ_{PL} (ns)	Viscosity (cP)	Reference
Glycerol	3.66	954	14
Ethylene glycol	2.99	16.790	14
Ethanol	3.2	1.074	15
Water	1.68, 1.65	0.890	14,16
Methanol	2.54	0.544	14
id.	~1.5*	0.544	17

* 2 photon excitation.

SI-III. Author Contributions

SC synthesized the nanocolloids, completed the TEM, SQUID and XRD characterizations. The toxicity study was completed by CH and LW. MPMD was more involved in the time resolved PL data while PA suggested the nanocolloids architecture, supervised the syntheses and characterizations, as well as tested the polymer pathway including functionalization and purification.

MPMD and PA jointly designed, coordinated the contributions of all the collaborators involved in the completion of the project. They also wrote the manuscript.

SI-IV. Notes and references

1 (a) S. Chen and P. André, *Int. J. nanoTech.* , 2012, **9**, 39; (b) M. Chen, J. P. Liu and S. H. Sun, *J. Am. Chem. Soc.*, 2004, **126**, 8394; (c) V. Nandwana, et al., *J Phys Chem C*, 2007, **111**, 4185; (d) H. N. McMurray and G. Williams, *J. Appl. Phys.*, 2002, **91**, 1673; (e) C.

Wang, et al., *Angew. Chem.-Int. Edit.*, 2007, **46**, 6333; (f) N. Poudyal, et al., *Nanotechnology*, 2008, **19**, 355601; (g) M. Delalande, et al., *J. Mater. Chem.*, 2007, **17**, 1579; (h) V. Monnier, et al., *Small*, 2008, **4**, 1139; (i) S. Chen, et al., *J Mat Chem*, 2010, **21**, 3646; (j) H. G. Bagaria, et al., *J Appl Phys*, 2007, **101**, 104310; (k) S. N. Shah, et al., *Dalton T*, 2009, 8479; (l) C. J. Xu, et al., *J Am Chem Soc*, 2009, **131**, 15346; (m) H. W. Gu, et al., *J. Am. Chem. Soc.*, 2005, **127**, 34; (n) M. Takahashi, et al., *J. Appl. Phys.*, 2005, **97**, 10J307; (o) S. S. Kang, et al., *Appl. Phys. Lett.*, 2005, **86**, 062503; (p) S. Chen, et al., *Cryst.Eng.Comm.*, 2011, **13**, 3330; (q) H. L. Nguyen, et al., *Chem. Mat.*, 2006, **18**, 6414; (r) Michael Bühl, Herbert Früchtl and P. André, *Chem. Phys. Lett.* , 2011, **509**, 158.

2 M. Chen, J. P. Liu and S. Sun, *J Am Chem Soc*, 2004, **126**, 8394.

3 Y. Tanaka and S. Maenosono, *J Magn Magn Mater*, 2008, **320**, L121.

4 R. Koole, et al., *Chem Mater*, 2008, **20**, 2503.

5 (a) H. Ow, et al., *Nano Lett.*, 2005, **5**, 113; (b) A. Burns, et al., *Small*, 2006, **2**, 723; (c) A. Burns, H. Ow and U. Wiesner, *Chem. Soc. Rev.*, 2006, **35**, 1028; (d) D. R. Larson, et al., *Chem. Mat.*, 2008, **20**, 2677.

6 A. Bonakdarpour, et al., *J. Electrochem. Soc.*, 2005, **152**, A61.

7 L. V. Azaroff, *Elements of X-ray Crystallgraphy*, McGraw-Hill, Inc., New York, 1968.

8 (a) D. C. Lee, et al., *J. Phys. Chem. B*, 2006, **110**, 11160; (b) T. Thomson, et al., *J. Appl. Phys.*, 2004, **95**, 6738.

9 S. Chen, et al., *J. Am. Chem. Soc.*, 2010, **132**, 15022.

10 (a) J. H. Gao, et al., *J. Am. Chem. Soc.*, 2008, **130**, 11828; (b) J. Gao, et al., *J Am Chem Soc*, 2007, **129**, 1428; (c) C. Xu, et al., *J.Am.Chem.Soc.*, 2009, **131**, 15346.

11 J. Choi, et al., 2007, **12**.

12 (a) M. A. Dobrovolskaia and S. E. McNeil, *Nat. Nanotechnol.*, 2007, **2**, 469; (b) R. Bakalova, et al., *Int. J. Nanomed.*, 2011, **6**, 1719.

13 J. R. Lakowicz, *Principles of fluorescence spectroscopy*, Kluwer Academic/Plenum, New York ; London, 1999.

14 T. L. Chang and H. C. Cheung, *J. Phys. Chem.*, 1992, **96**, 4874.

15 I. B. Berlman, *Handbook of fluorescence spectra of aromatic molecules*, Academic Press, New York, 1971.

16 ISS, http://www.iss.com/resources/fluorophores.html, 2008.

17 R. K. P. Benninger, et al., *Anal. Chem.*, 2006, **78**, 2272.